CONTENTS

TABLES

FIGURES

APPENDICES

4.6 Geology and Seismicity

4.6.1 Regional Geology

The Amulsar gold and silver deposit is situated in south-central Armenia and is hosted in an Upper Eocene to Lower Oligocene calc-alkaline magmatic-arc system that extends south-west through southern Georgia into Turkey, and south-east into the Alborz-Arc of Iran. The geological structure of Armenia within the Lesser Caucasus is illustrated by Hässig et al (2013)[1] (reproduced in Figure 4.6.1). This map illustrates that at a regional scale the area to the north and east of the Amulsar Mountain project is occupied by recent (Pliocene and Quaternary) sediments and volcanites (igneous rocks and volcanogenic sediments), indicating that older units encountered in the vicinity of Amulsar Mountain do not outcrop in the Syunik Massif further eastward from the Study Area (GSA). The Project area is not within the major zones of tectonic activity in Armenia. However, geologically young basalt scoria cones within the Project area indicate that the area is geologically active.

Volcanic and volcano-sedimentary rocks of this system comprise a mixed marine and terrigenous sequence that developed as a near-shore continental arc between the southern margin of the Eurasian Plate and the northern limit of the Neo-Tethyan Ocean. In the Early Oligocene, the Neo-Tethyan Ocean closed, and subduction ceased along this margin when a fragment of continental crust, known as the Sakarya continent, collided at the trench axis and accreted with the Eurasian plate. The location of Amulsar within this arc is shown in Figure 4.6.2.

[1] Linking the NE Anatolian and Lesser Caucasus ophiolites: evidence for large-scale odbuction of oceanic crust and implications for the formation of the Lesser Caucasus-Pontides Arc. Hassig, M; Rolland, Y; Sosson, M, Galoyan, G; Sahakyan, L; Topuz, G; Celik, O; Avagyan, A and Muller, C. 2013.

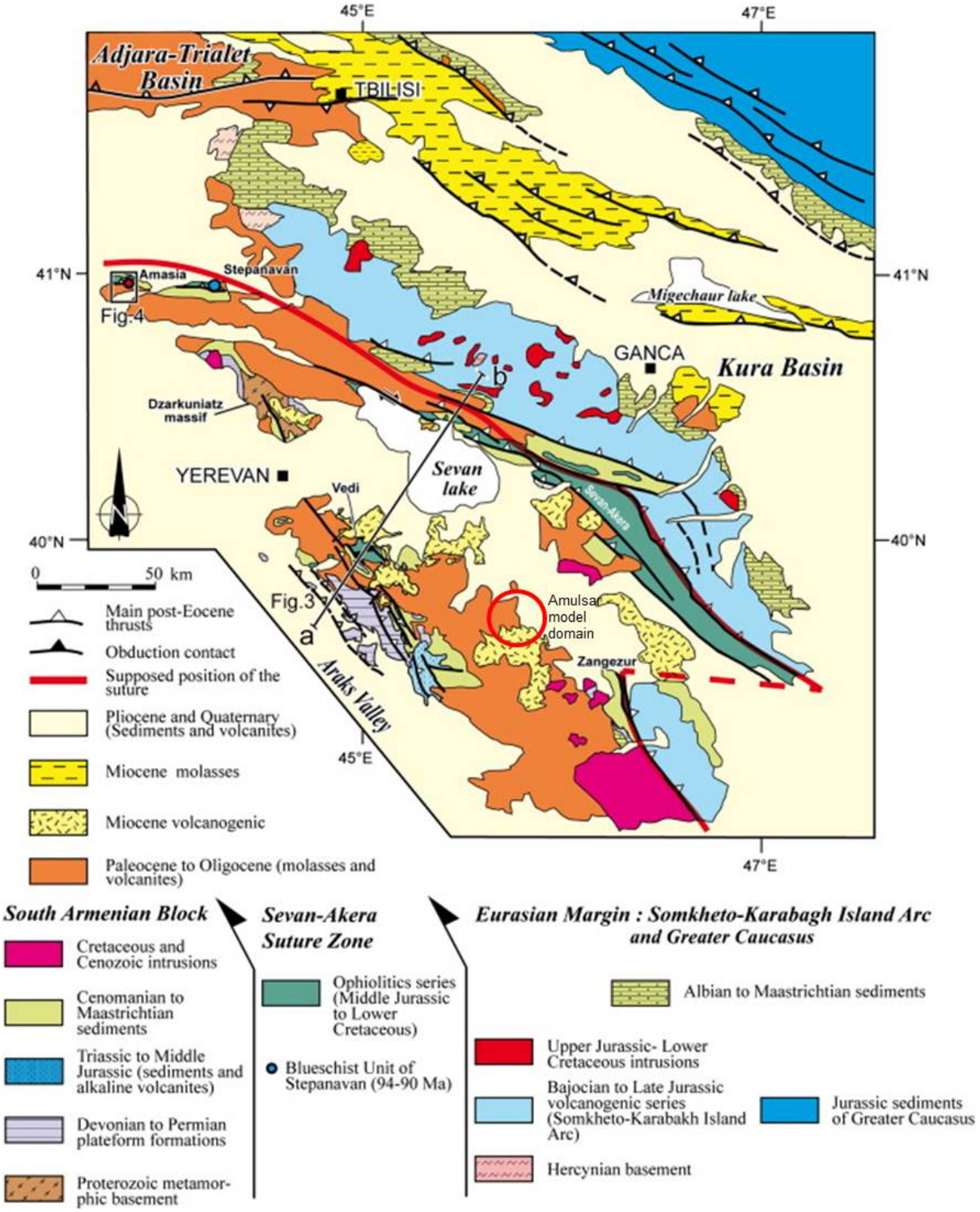

(note: for ease of reading this figure has also been duplicated as Figure 4.8.1)

Figure 4.6.1: Structural map of the Lesser Caucasus

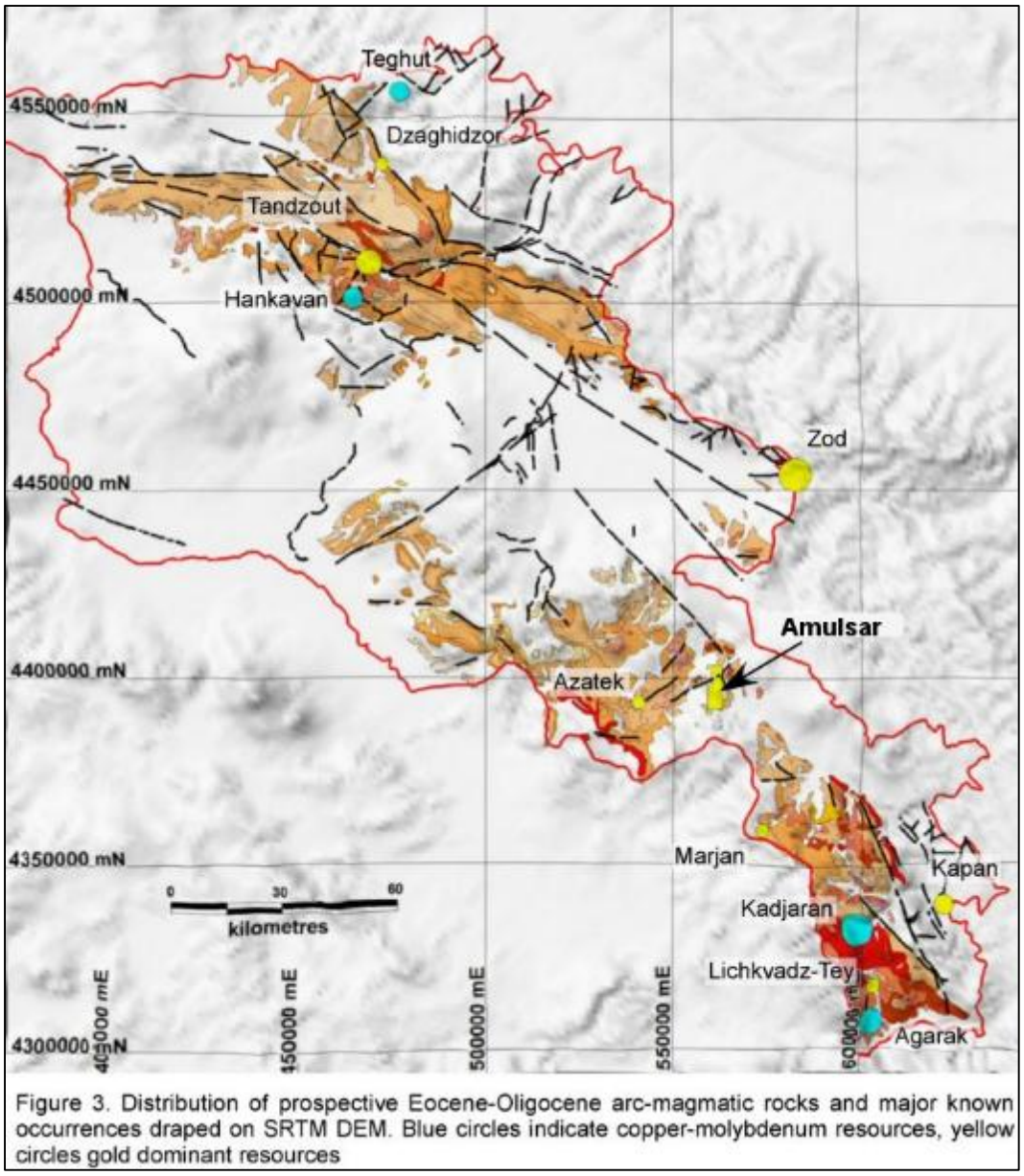

Figure 3. Distribution of prospective Eocene-Oligocene arc-magmatic rocks and major known occurrences draped on SRTM DEM. Blue circles indicate copper-molybdenum resources, yellow circles gold dominant resources

Source: *Lydian, 2013*

Figure 4.6.2: Regional Geology, Upper Eocene to Lower Oligocene Calc-Alkaline Magmatic Arc System

4.6.2 Local Geology

The geological model of Amulsar is based on a division of the geological sequence into two units:

- The Amulsar Mountain upper volcano-sedimentary sequence – "Upper Volcanics" (VC) comprising weakly bedded volcanogenic feldspathic quartzite interbedded with abundant thin and thick lenticular masses and flow masses, andesitic volcanic flows

and volcanic breccia which are strongly silicified throughout, with strong alunite alteration.

- The Amulsar Mountain lower volcano-sedimentary sequence – "Lower Volcanics" (LV), at higher altitudes this unit comprises predominantly pervasively argillically altered porphyritic andesite, most likely dominantly sub-volcanic intrusives (Lydian et al, 2013)[3]. However, it also incorporates the regional Palaogene volcano-sedimentary sequence described above, in which volcanic and volcaniclastic units are only sparsely interspersed lower in the stratigraphy.

The Upper Volcanics outcrop on Amulsar Mountain and on the eastern mountain flank. The Lower Volcanics outcrop to the west of the mountain and occur underlying other units at lower elevations surrounding the mountain. The Lower Volcanics are extremely thick, outcropping from high elevations on the west of Amulsar Mountain (above 2700 m asl) to below 1400 m asl in the gorge of the Arpa River, indicating a total thickness of more than 1300 m.

At lower elevations to the east and west of Amulsar Mountain ridge, and covering the northern face of the ridge, unaltered Cenozoic Flow Basalts overlie the Palaeogene volcano-sedimentary and intrusive rocks forming plateaus along the banks of the Vorotan River and Arpa River gorges.

The Amulsar deposit lies within a thick package of Paleogene volcano-sedimentary rocks. Locally, these rocks flanking Amulsar consist of multiple fining-upward cycles of volcanogenic conglomerate and mass flow breccia fining-upward to volcanogenic and marly mudstones to thin calcilutite limestone. Andesitic to dacitic volcanic and volcaniclastic units are sparsely interspersed low in the stratigraphy, but increase in frequency as higher stratigraphic levels are exposed on the flanks of the Amulsar ridge. Strata peripheral to the deposit are sub-horizontal to gently dipping, with little internal structure except where cut by steep faults.

The Amulsar deposit is hosted within the Amulsar Ridge; the ridge trends north-northeast for about 5 km and rises to a height of 1,000 m from the surrounding land (see Figure 4.6.3). The ridge is a geologically anomalous feature comprising volcano-sedimentary rocks that while broadly similar to lower structural elevations contains a larger component of lenticular mass flow deposits. The Amulsar deposit is associated with a complex alteration system and a

structural complexity that has not been observed in this sub-region. Flanking the deposit is an anomalous cluster of small plutonic and subvolcanic intrusives.

The main rock units recognized by Lydian at the Amulsar project are summarised below (see also Figure 4.6.3 and cross sections on Figure 4.6.4

Upper Volcanics (VC). Sparsely bedded volcanogenic conglomerate, feldspathic sandstone and minor siltstone are interbedded with abundant thin and thick lenticular mass wasting (debris flow) units; minor andesitic flow volcanics and volcanogenic/volcaniclastic breccia. Debris flow units are dominated by pebble and cobble breccia with sparse large boulder components. Significantly, clasts in some of the mass-flow breccias appear to have been silicified prior to deposition. Examples of representative lithologies for VC are provided in Figure 4.6.5

Lower Volcanics (LV). Strong argillic alteration strongly masks the protolith of these rocks, but the dominant rock type is a feldspar-porphyritic andesite, generally without any flow alignment or other flow characteristics. Some rocks contain hornblende phenocrysts. These rocks are most likely subvolcanic intrusives. Locally they contain silicic volcanic fragments or possible xenoliths. Minor pebble to cobble fragmental rocks and indeterminate rock types also occur, as well as minor feldspar-amphibole porphyritic andesite and a single reported occurrence in drill core of amphibole-magnetite andesite. Examples of representative lithologies for LV are provided in Figure 4.6.5

Local intrusive suites. Two different intrusive suites occur within or adjacent to the licence area: small, radiometrically above background, fresh-looking silicic plutons (micro-leucogranite; quartz monzonite); and an extensive suite of slightly altered, quartz-poor, intermediate plutons and subvolcanic dykes (diorite, monzonite porphyritic andesite) that are characteristically magnetite-bearing. The latter are in contact only with argillically altered rocks of the Lower Volcanics; whereas one of the fresh silicic plutons is surrounded by Upper Volcanics. Some of the dykes have similar porphyritic textures to the clay-altered intrusive andesite within the Upper Volcanics, although any connection has not been established.

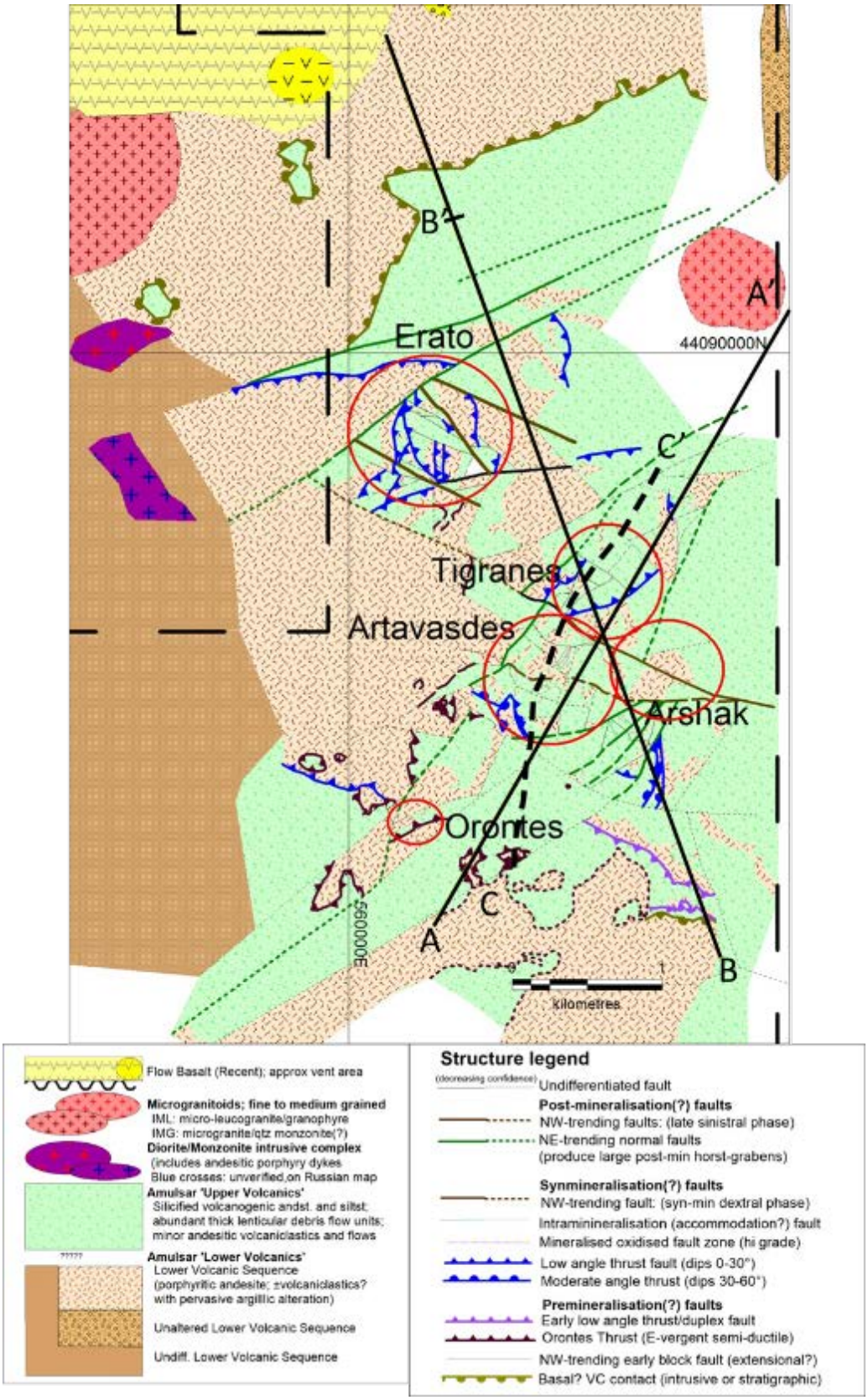

Source: *Lydian, 2013*

Note: Cross-section lines shown on map

Figure 4.6.3: Geological Map of Amulsar Project

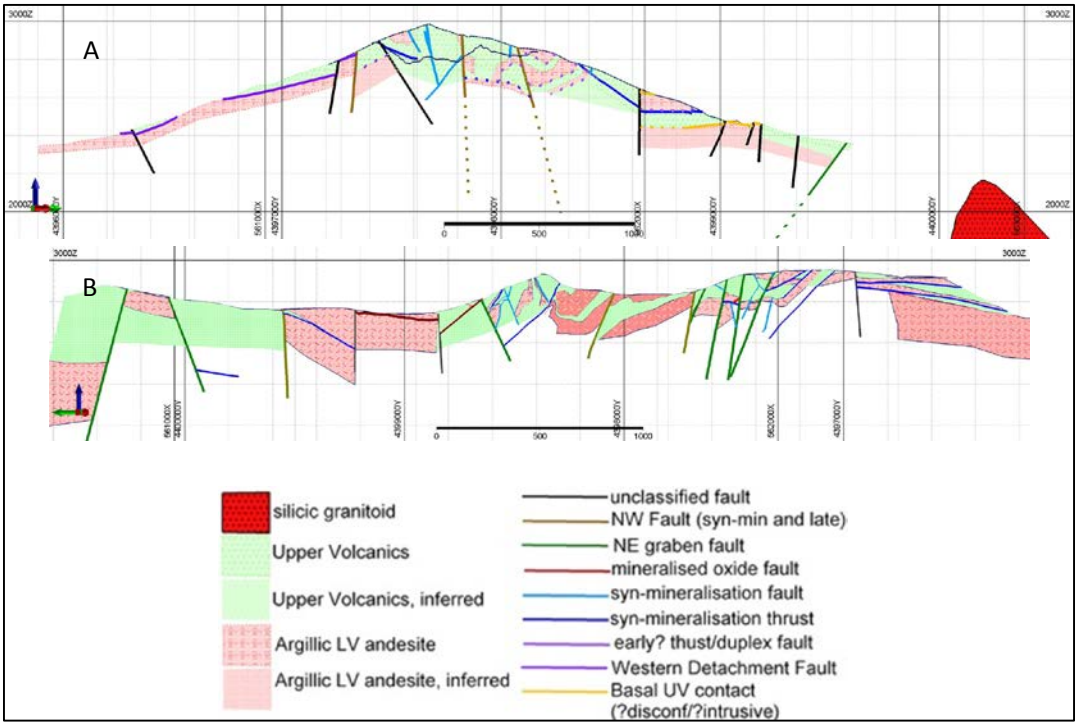

Figure 4.6.4: Amulsar Geological Cross-sections A-A' and B-B'

Alteration

The LV unit is characterized by pervasive argillic alteration in the region of the resource. However, this alteration reduces toward the periphery of the licence area. The argillic alteration is commonly void of gold mineralisation, other than at a contact with the VC unit, or occasionally where through-going faults crosscut the LV unit. In both cases, a marked increase in iron-oxide and weak silicification can also be observed. Alteration within the VC unit is predominantly massive silica or silica-alunite, forming the main host to gold mineralisation. The pervasive argillic alteration of the Lower Sequence appears to be cut by the disconformity, which implies that the two alteration styles are unrelated in time.

Source*: Lydian, 2014.*
a. VC unit, polymictic conglomerate fining upwards to laminated sandstone with small basal loading structures in the overlying conglomerate, west Artavazdes. **b.** VC unit, polymictic matrix supported breccia (primary or volcaniclastic), north Tigranes. **c.** LV unit, strongly altered feldspar-phyric andesite, west Artavazdes. **d.** LV unit, moderately altered feldspar-hornblende porphyritic andesite from core sample, Artavazdes.

Figure 4.6.5: Representative Rock Types of the Amulsar Deposit

Structure

Within the confines of the Amulsar Ridge a structural complexity exists whereby dips become steep and overturned. At least four different sets of structure (shears, folds, and faults) produce the final geometry, with increasingly brittle response in the younger structures. Thick slabs of Lower Volcanics arch into an antiform, before a transition across faults into the highly complex central folded zone. Within the complex zone, the andesitic slabs are more numerous and thinner. The overall pattern appears to be a footwall synform possibly below a southeast-vergent thrust. The formation of the multiple thin panels in the complex zone is that they may be the result of duplexing during this major thrust event. Although mineralization occurs within the complex zone in the core of this large apparent fold structure, it is the further complexity produced by the refolding of an already folded structure that creates the final host structure. Gold mineralization is intimately associated with the variably oriented accommodation faults and the large volume of fractured mineralized rock that links them. These fractures are small-scale accommodation structures that allow local deformation associated with the folding.

Mineralisation

Gold mineralisation at Amulsar is thought to have been a late event in the development of the deposit, occurring dominantly within the silica-alunite-altered volcano-sedimentary breccia units of the VC unit. Mineralisation is also associated with iron oxide-coated fracture surfaces, and heavily oxidized faults that cut the silica-alunite alteration. Based on a structural study of the deposit by Holcombe (2013)[2], gold mineralisation is believed to be associated with iron oxide coatings, fillings, and hydraulic breccias in late stage brittle fractures and faults within a thrust and fold complex.

Three dominant controls of mineralisation have been identified to include the following:

- Faults and fractures acting as conduits for mineralizing fluids, resulting in gold mineralisation as gossanous veins that form broad corridors of closely-spaced high-grade structures;
- Porous and permeable lithological units, including hydrothermal breccias, volcaniclastic breccias, leached vuggy volcanics – allowing lateral migration of fluids away from structurally controlled conduits; and
- Relatively impermeable argillic altered LV rocks formed an impermeable boundary along contact zones with VC rocks, causing 'ponding' of higher-grade gold mineralisation along contacts, often forming as leached or gossanous zones.

Examples of gold mineralisation in the drill core are shown in Figure 4.6.6

Silver mineralisation is also present at Amulsar, but the genesis and distribution of it is not well understood. Silver mineralisation does not correlate with gold mineralisation. Average silver grades range from 2 g/t to 5 g/t and locally can occur in the 100 g/t to 200 g/t range.

A small silver mining project adjoins the Amulsar licence to the north-west, exploiting a structurally controlled argentiferous galena vein. This deposit is located at a lower stratigraphic level than the Amulsar deposit.

[2] Holcombe, R., 2013. Amulsar 3D Geological Model Revision: Summary and Resource Implications November 2013

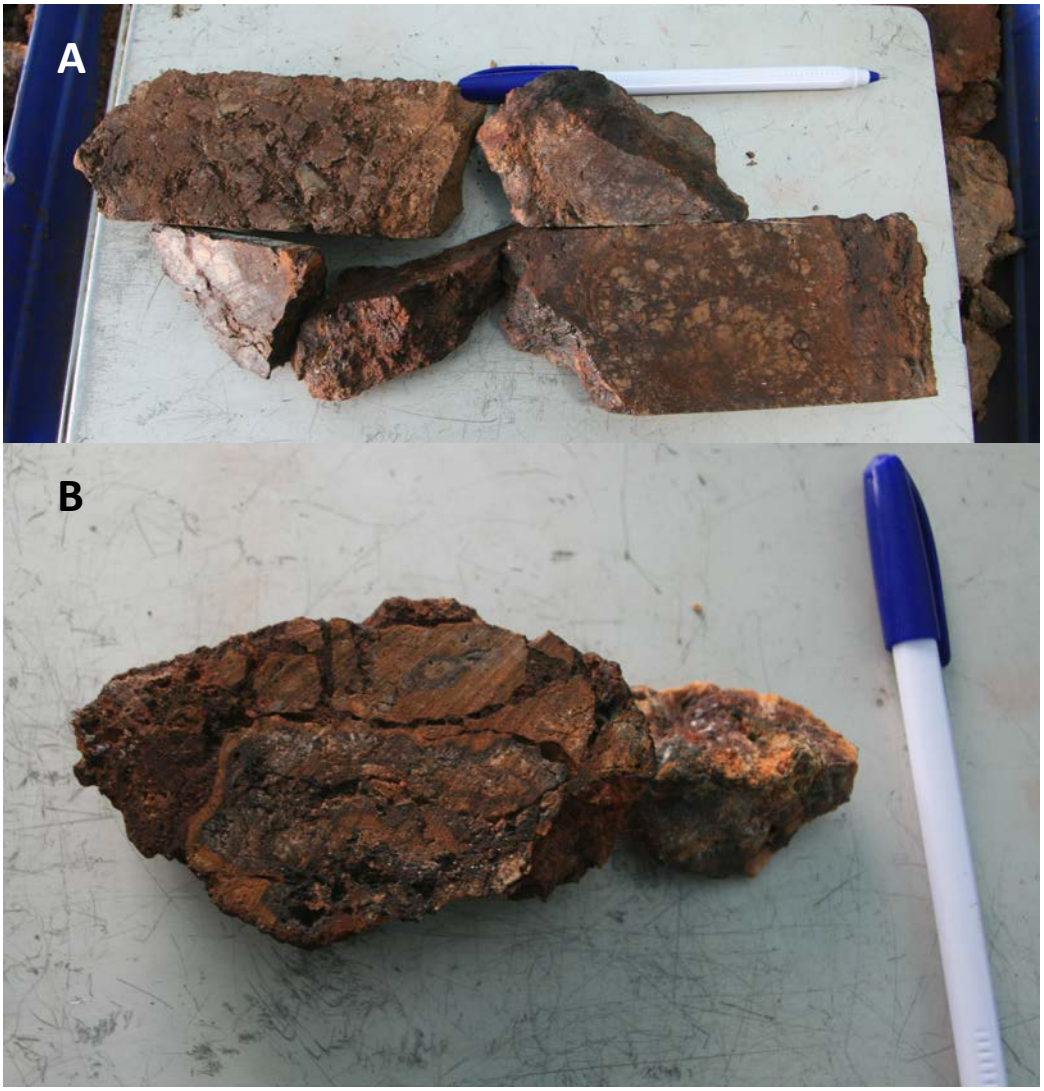

Notes:
A: Brecciated VC unit, highly altered, strong iron oxidization, 96.1 to 96.5 m, 96.0-97.0 at 5.67 g/t Au.
B: Brecciated VC unit, highly altered, strong iron oxidization, 97.0 to 97.1 m, 97.0-98.0 at 13.7 g/t Au.

Figure 4.6.6: Examples of Gold Mineralisation in Core Samples, Drill hole DDA-047

Ore Mineralogy

The mineralogy of the ore bearing silicified Upper Volcanic unit is very simple, predominantly composed of quartz (typically 60-98%). Fractures and vesicles are infilled with goethite, limonite and haematite and it is within this oxide infill that the gold mineralization occurs. Minor/trace amounts of potassium-feldspar, rutile, chlorite, mica, alunite and jarosite have also be found within the unit.

The gold mineralization modelled at Amulsar is associated with oxide fracture fills and the ore that has been evaluated in the current resource model is oxide in its natural state. Table 4.6.1

illustrates a set of typical ore whole rock analyses conducted by Kappes Cassidy Associates (KCA) from the 2012 Amulsar metallurgy testwork programme.

Table 4.6.1: Whole rock analysis of ore composites (KCA 2012)

Constituent	Unit	KCA Composite No. 61768 DDAM-130	KCA Composite No. 61769 DDAM-137	KCA Composite No. 61770 DDAM-140	KCA Composite No. 61771 DDAM-148	KCA Composite No. 61772 DDAM-169	KCA Composite No. 61773 DDAM-174
SiO2	%	80.59	85.41	84.52	93.74	91.3	68.4
Si	%	37.68	39.93	39.51	43.82	42.68	31.98
Al2O3	%	3.33	1.38	0.92	0.8	0.93	8.96
Al	%	1.76	0.73	0.49	0.42	0.49	4.74
Fe2O3	%	8.53	8.91	10.1	2.59	4.65	8.83
Fe	%	5.97	6.23	7.06	1.81	3.25	6.17
CaO	%	0.05	0.03	0.03	0.02	0.02	0.1
Ca	%	0.04	0.02	0.02	0.01	0.01	0.07
MgO	%	0.04	0.01	0.02	0.02	0.02	0.05
Mg	%	0.02	0.01	0.01	0.01	0.01	0.03
Na2O	%	0.12	0.09	0.06	0.05	0.04	0.37
Na	%	0.09	0.07	0.04	0.04	0.03	0.27
K2O	%	0.62	0.19	0.09	0.08	0.07	1.33
K	%	0.51	0.16	0.07	0.07	0.06	1.1
TiO2	%	1.46	1.31	1.28	1.43	1.21	1.18
Ti	%	0.88	0.79	0.77	0.86	0.73	0.71
MnO	%	<0.01	<0.01	<0.01	0.01	0.02	0
Mn	%	0	0	0	0	0	0
SrO	%	0.03	0.01	<0.01	<0.01	<0.01	0.07
Sr	%	0.03	0.01	0	0	0	0.06
BaO	%	0.04	0.01	0.09	0.02	0.01	0.1
Ba	%	0.04	0.01	0.08	0.02	0.01	0.09
Cr2O3	%	0.02	0.01	0.02	0.02	0.02	0.02
Cr	%	0.01	0.01	0.01	0.01	0.01	0.01
P2O5	%	0.1	0.02	0.02	0.01	0.02	0.21
P	%	0.04	0.01	0.01	0	0.01	0.09
LOI1090°C	%	4.9	2.47	2.46	1.09	1.66	10.22
SUM	%	99.83	99.85	99.61	99.88	99.97	99.84

Barren Rock Mineralogy

There are three potential streams of Barren Rock that have been identified in the Mining Schedule (see also Figure 4.6.3 and Figure 4.6.4; these are Upper Volcanics that do not meet cut-off grade, Lower Volcanics and Colluvium. The three different waste materials have been subjected to a mineralogical evaluation based on x-ray diffraction (XRD) and microscopy (GRE, 2014). Based on this analysis, the summary of the mineralogy is as follows:

- **Lower Volcanics** - In ten LV samples, quartz is present in all samples in amounts ranging from 20 to 77 percent, plagioclase is present in two samples at 8 and 66 percent, pyrite in five samples ranging from trace to 24 percent, alunite in four samples at 6 to 53 percent, natroalunite in a single sample at 45 percent, jarosite in two samples ranging from trace to 10 percent, goethite in a single sample at 2 percent, hematite in four samples ranging from trace to 9 percent, sericite/illite in four samples ranging from trace to 30 percent, illite/smectite in two samples with values of 3 and 5 percent, smectite in a single sample at 1 percent, adularia in two samples with values of 2 and 3 percent, and chalcopyrite, iron oxide, rutile, and gold in varying numbers of samples at trace levels.
- **Upper Volcanics** - In seven VC samples, quartz is present in all samples in amounts ranging from 27 to 99 percent, feldspars are absent from all samples, pyrite is present in four samples at trace levels, alunite in three samples at 9 to 70 percent, jarosite in two samples at trace and 10 percent, goethite in a single sample at 15 percent, hematite in five samples ranging from 1 to 10 percent, hematite/goethite in one sample at 3 percent, adularia in three samples ranging from 1 to 5 percent, rutile in six samples ranging from trace to 2 percent, and chalcopyrite and iron oxide in a small number of samples at trace levels.
- **Colluvium** - In three colluvium samples, quartz is present in all samples in amounts ranging from 57 to 88 percent, feldspars are absent, pyrite is present in all samples at trace levels, chalcopyrite is present in two samples at trace levels, alunite in two samples at trace and 30 percent, jarosite in one sample at 2 percent, hematite in three samples at 3, 3, and 8 percent, adularia in three samples at 1, 2, and 3 percent, kaolinite in two samples at 7 and 30 percent, rutile in three samples all at 1 percent, and gold in two samples at trace levels.

Table 4.6.2 and Table 4.6.3 illustrate the X-Ray Diffraction results for 21 samples of barren rock[3].

Table 4.6.2: X-Ray Diffraction (XRD) and Petrography Tigranes/Artavasdes Barren Rock Samples (GRE 2014)

Mineral	Chemical Formula	Lower Volcanics						Upper		
		ARD	ARD	ARD	ARD	ARD	ARD	ARD	ARD	ARD
Plagioclase	NaAlSi3O8 – CaAl2Si2O8	--	--	66	--	--	--	--	--	--
Quartz	SiO2	46	55	20	35	49	75	86	99	27
Alunite	KAl3(SO4)2(OH)6	--	--	--	53	--	21	9	--	70
Natroalunite	NaAl3(SO4)2(OH)6	--	45	--	--	--	--	--	--	--
Goethite	FeOOH	--	--	--	--	--	--	--	--	--
Hematite	Fe2O3	--	--	--	trace	--	3	3	--	--
Hematite/Geo	FeOOH - Fe2O3	--	--	--	--	--	--	--	--	3
Iron Oxide	FeO	--	trace	1	--	--	--	--	trace	--
Rutile	TiO2	4	trace	<1	trace	--	1	2	trace	--
Pyrite	FeS2	10	--	8	--	10	--	--	--	--
Sericite/Illite	K0.5-1(Al,Fe,Mg)2(SiAl)4O10(OH)2 nH2O -									
	(K,H3O)(Al,Mg,Fe)2(Si,Al)4O10[(OH)2,(H2O)]	17	<1	4	--	30	--	--	--	--
Kaolinite	Al2Si2O5(OH)4	23	--	--	12	11	--	--	--	--
Smectite	(Na,Ca)(Al,Mg)6(Si4010)3(OH)6-nH20	--	--	1	--	--	--	--	--	--

[3] Amulsar Project geochemical characterisation and prediction report – update (GRE, 2014)

Table 4.6.3: X-Ray Diffraction (XRD) and Petrography Erato Barren Rock Samples (GRE 2014)													
Mineral	**Chemical Formula**	**Lower Volcanics**					**Upper Volcanics**				**Colluvium**		
		BR-SMA-	**VC-SV-**	**LV-ARGC-**	**LV-ARGC-**	**LV-ARGC-**	**BR-SM-**	**BR-SMV-**	**VC-SA-**	**LV-SA-**	**COL-SM-**	**COL-SA-**	**COL-UN-**
Plagioclase	NaAlSi3O8 – CaAl2Si2O8	--	--	8	--	--	--	--	--	--	--	--	--
K-Feldspar	KAlSi3O8	--	--	--	--	--	--	--	--	--	--	--	--
Quartz	SiO2	77	65	53	45	65	40	97	89	53	63	57	88
Alunite	KAl3(SO4)2(OH)6	17	6	--	--	--	22	--	--	--	30	--	Trace
Natroalunite	NaAl3(SO4)2(OH)6	--	--	--	--	--	--	--	--	--	--	--	--
Goethite	FeOOH	2	--	--	--	--	--	--	--	15	--	--	--
Hematite	Fe2O3	2	6	--	--	9	8	1	5	10	3	8	3
Hematite/Geo	FeOOH - Fe2O3	--	--	--	--	--	--	--	--	--	--	--	--
Iron Oxide	FeO	--	--	--	--	--	--	--	--	--	--	--	--
Rutile	TiO2	Trace	--	1	1	1	Trace	Trace	1	1	1	1	1
Pyrite	FeS2	Trace	--	Trace	24	--	Trace	Trace	Trace	Trace	Trace	Trace	Trace
Chalcopyrite	CuFeS2	Trace	--	--	--	--	--	--	Trace	Trace	Trace	--	Trace
Pyrrhotite	FeS	--	--	--	--	--	--	--	--	--	--	--	--
Gold	Au	--	--	Trace	--	--	--	--	--	--	Trace	Trace	--
Sericite/Illite	K0.5-												
	(K,H3O)(Al,Mg,Fe)2(Si,Al)4O10[(	--	--	--	--	25	--	--	--	--	--	--	--
Kaolinite	Al2Si2O5(OH)4	--	20	25	25	--	30	--	--	10	--	30	7
Adularia	KAlSi3O8	2	3	--	--	--	--	2	5	1	3	2	1
Jarosite	KFe3(OH)6(SO4)2	Trace	--	10	--	--	Trace	--	--	10	--	2	--
Illite/Smectite	(K,H3O)(Al,Mg,Fe)2(Si,Al)4O10[(	--	--	3	5	--	--	--	--	--	--	--	--
Smectite	(Na,Ca)(Al,Mg)6(Si4010)3(OH)6-	--	--	--	--	--	--	--	--	--	--	--	--

The VC is non-acid-generating (NAG) even though some samples contain trace pyrite and the majority of the samples are devoid of neutralization potential. Leachate from VC rocks does not pose a material water quality risk. Therefore, the rock can be safely used as an aggregate for construction, drainage, or to from the "shell" to construct encapsulation cell. The high degree of silicification gives this rock resistance to chemical and mechanical weathering.

The LV barren rock is potentially acid-generating (PAG). However, there is a wide range of sulphide concentrations in the LV, and many LV samples do not produce moderate to severe acidic leachate (defined as a cell with leachate with pH<4.0 and sulphate concentrations >100 mg/L) despite long-term humidity cell testing. The Amulsar LV barren rock has resistance to the formation of ferric iron oxidation conditions even when placed in a humidity cell. On-site kinetics, as exhibited at the historic mine waste piles, suggests that ferric iron oxidation has not taken place despite decades of reaction time.

Metals leaching occurs in strongly acidic conditions (which, as previously identified, are rare in this rock type).

Overall, the Amulsar LV formation would be acid-generating and there is the risk that exposed rock has the potential to degrade water quality by suppressing pH, and by possessing elevated sulphate, iron, copper, selenium, or manganese concentrations.

Schedule of NAG and PAG waste

For the life of the Project, it is envisaged that 60% of the barren rock excavated will be non-acid generating (NAG) Upper Volcanics and colluvium, with 40% being potentially acid generating (PAG) Lower Volcanics. Based on the current Amulsar lithology model, barren rock types were defined in the mining schedule by lithology. The volumes of expected NAG and PAG barren rock are shown by mining period in Table 4.6.4.

Table 4.6.4 In-Situ Volumes of Waste Type by Mining Period			
	Colluvium	**NAG Barren Rock (VC)**	**PAG Barren Rock (LV)**
Period	000's t	000's t	000's t
Year -1	26	699	259
Year 1	175	11,035	7,930
Year 2	373	16,214	7,246
Year 3	291	17,397	10,420
Year 4	438	12,381	11,027
Year 5	399	18,085	8,440
Year 6	18	18,980	2,733
Year 7	273	12,361	11,631
Year 8	318	15,453	17,304
Year 9	0	10,935	12,895
Year 10	0	2,714	635
Total	**2,311**	**136,253**	**90,521**

The NAG/PAG barren rock schedule has been taken into account with the detailed scheduling of encapsulation in the BRSF[4].

Location of Project ancillary infrastructure (see Figure 4.6.7)

Crusher and maintenance

The area selected for the location of the crusher building and associated ramps and connecting conveyors is situated within basaltic lave flow units. There are no potentially mineralised units within the construction footprint required for ore crushing operations. It should be noted that the location of the BRSF also does not host any potentially mineralised units.

HLF and associated infrastructure

The HLF is located at a lower elevation than the open pits and is connected by overland conveyor from the crushing plant. The footprint of the HLF is located on bedrock consisting of an unaltered andesitic volcaniclastic unit. The proposed ADR plant is also located on the andesite unit. Cores removed from the boreholes have been sampled for sterilisation

[4] Ibid. 3, p4.6.13

assessment. This analysis has confirmed that the mineralised units of the Amulsar deposit do not extend into this area.

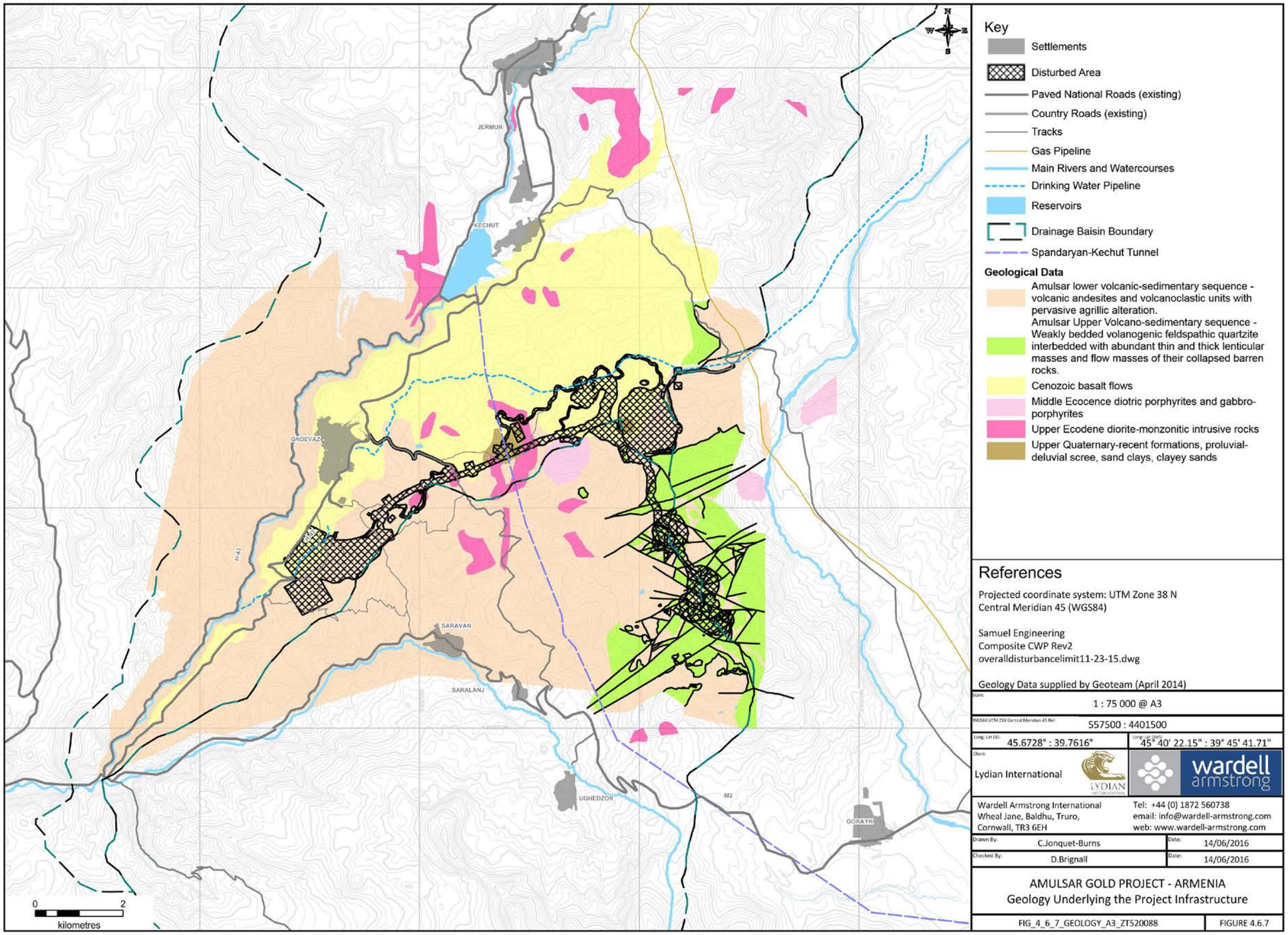

Figure 4.6.7: Geology Underlying the Project Infrastructure

4.6.3 Superficial Deposits

The Project and surrounds was glaciated during the Quaternary. Soils are generally absent at high elevations and are poorly developed on lower mountain slopes. Significant superficial deposits (2m to 10m) are limited to sheltered landforms and lower elevations of the Project and are largely comprised of clay, gravelly clay and clayey gravel with occasional cobbles to boulders of basalt.

Substantial clay deposits are present in the licence area. Widespread clays are thought to be derived from the breakdown of underlying fractured andesite. Localised clay deposits are also found, for example within glacial landforms. These may be lacustrine in origin, forming after volcanic events and flows dammed surface water channels. These clays, such as those beneath the proposed BRSF, are green in colour, indicative of high volcanic ash content. Gravelly clays of up to 15 m thickness were encountered at the centre of the BRSF.

Alluvium (clay, sandy clay and sand) underlies river catchment areas, including the eastern edge of the BRSF, to a depth of approximately 13 m. Bedrock exposures are evident in the Vorotan River; however, alluvial deposits in the Vorotan valley have been confirmed to approximately 8 m below ground level (bgl). Clayey basalt gravels are present up to 26 m bgl in the Vorotan plain. In summary superficial glacial and river flood deposits of up to 30 m thickness underlying the Vorotan plateau in the licence area.

4.6.4 Tectonics and Seismicity

The Project licence is located within a seismically active region of the Arabia-Eurasia plate boundary zone. This plate boundary is a continent-continent collision zone, and studies undertaken by Golder Associates (see Appendix 4.6.1) have shown that there are 17 fault zones with a total of 53 fault segments within approximately 250km of the project site.

Golder's field investigations and review of available literature and satellite imagery found no geomorphic evidence for the trace(s) of faults or other tectonic geomorphology within the Project area, including the proposed sites of the BRSF, HLF, crushing plant, or open pit. There is thus a very low potential for surface fault rupture within the Project.

The Medvedev-Sponheuer-Karnik (MSK) intensity scale widely used in the Former Soviet Union (FSU) is somewhat similar to the Modified Mercalli (MM) scale used today in the United States. Historical records show that there have been 107 relatively well-documented, strongly

felt earthquakes in the RA that have occurred from 600 B.C to 2003[5], the latter is the date of the last, intense earthquake in the RA. Historical records suggest that in the last 900 years the site has experienced strong to very strong (MSK VI to VII) perceivable shaking at least 3 times. Such perceivable shaking can cause Light to Moderate potential damage[6]. Historic earthquakes and seismic sources in relation to the Project are demonstrated in Figure 4.6.8

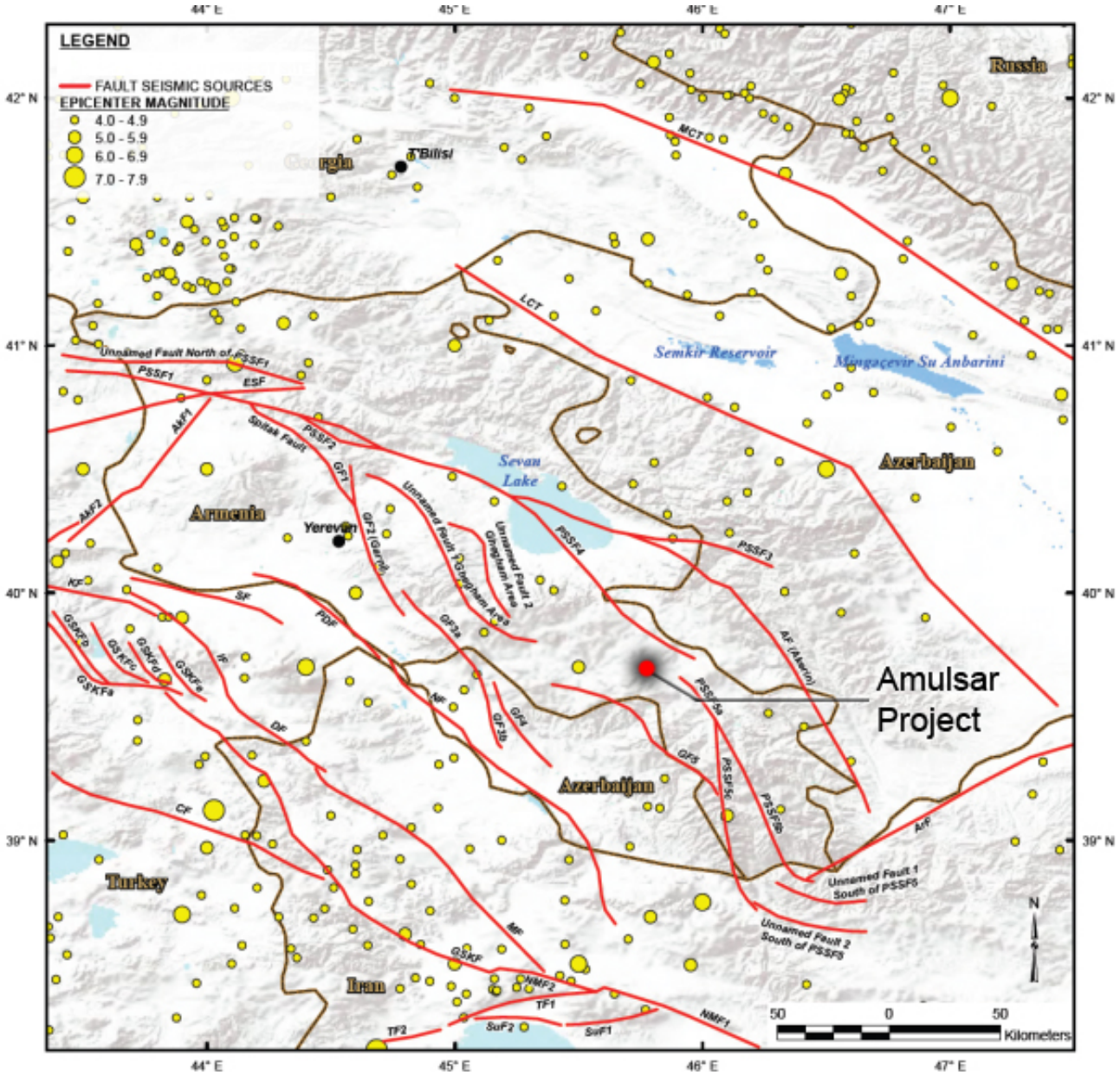

Figure 4.6.8: Historic Earthquakes and Fault Seismic Sources[6]

[5] Babayan, T., 2006, Atlas of strong earthquakes of the Republic of Armenia, Artsakh and adjacent territories from Ancient Time to 2003, National Academy of the Sciences republic of Armenia. 139pp

[6] http://earthquake.usgs.gov/earthquakes/shakemap/global/shake/b0008649/download/tvguide.txt

The 'Pambak-Sevan-Sunik fault Segment 4' (Figure 4.6.8) is located approximately 10km north of the Project licence, and has been calculated to have an average horizontal slip rate of 1.55mm/yr. Based on a seismo-tectonic model it was calculated that the estimated maximum magnitude earthquake from this fault segment would be in the region of M 7.2 (M is the moment magnitude scale, which is essentially the equivalent on the Richter Magnitude Scale).

A probabilistic seismic hazard analysis (PSHA) was conducted for the Project site. PSHA estimates the likelihood that the specified earthquake ground motions will be exceeded during a specified time. The likelihood of being exceeded is determined based on the probability of occurrence of all earthquakes at different locations on each significant seismic source, and the rate at which ground motions attenuate away from the earthquake source.

The PSHA assumed a 10% probability of occurrence over a 50-year time period, which results in the prediction of the effective probability of an event with a 475-year return period[7]. A moderate level of seismic hazard (475-year peak ground acceleration value (PGA)[8] of 0.20 to 0.34 g) has been assigned to the licence area based on the PSHA.

4.6.5 Acid Rock Drainage Characterisation

The characterization of the Acid Rock Drainage (ARD) properties of the Amulsar site was first reported by Golder Associates (see Appendix 8.19). This report has been fully-updated by GRE3 to include the results of additional geochemical testing, and to report predictive modelling associated with the up-to-date mine planning and ARD mitigation measures (see ARD Management Plan). The following sections present a summary of the revised geochemical characterization results.

Static testing of Mine Waste

Static testing defines the ARD-generation and metals leaching potential of a given rock type. The following static geochemical testing was performed on the rock types at the Amulsar Project.

[7] http://www.irmi.com/expert/articles/2003/gould07.aspx
[8] Global Seismic Hazard Assessment Programme (1999), http://www.seismo.ethz.ch/static/GSHAP/

Table 4.7.1: Static Geochemical Testing Program						
Material Type	**ABA**	**NAG pH Testing**	**Bulk Chemistry**	**Mineralogy**	**SPLP Effluent Testing**	**NAG Effluent Testing**
Barren Rock - Tigranes/ Artavazdes	154	-	97	8	8	8
Barren Rock - Erato	80	50	42	12	9	12
Spent ore - Tigranes/ Artavazdes	6	-	-	-	6	-
Spent ore - Erato	7	7	7	-	7	7
Borrow materials	5	5	5	-	5	5

Where:

- ABA: Acid Base Accounting by Modified Sobek
- NAG pH: Net Acid Generating pH test
- Bulk Chemistry: mineral composition by ICP-MS whole rock analysis
- Mineralogy: Mineralogy evaluation via XRF followed by mineralogical analysis.
- SPLP effluent: Synthetic Precipitation Leaching Procedure
- NAG Effluent: Testing of the NAG pH effluent.

The characterization of rock types revealed the following:

- The VC is non-acid generating, despite the existence of trace AP;
- The VC has leachate slightly lower than circumneutral, likely due to the weathering of alunite. The weathering of alunite is not significant to water quality due to the very slow reaction kinetics and low total acidity produced;
- The LV is acid generating, but appears to be resistant to ferric iron oxidation under field conditions;
- Colluvium is not acid generating; and
- There is potential for metals leaching for copper, iron, manganese, selenium, and sulphate.

4.7.1 Acid-Base Accounting: Barren Rock

Acid Base Accounting (ABA) is a method by which the total potential for acid generation for a rock sample is compared to the total neutralization potential. It is an industry-standard method for determining the potential for acid generation in a rock type. Table 4.7.2 has a summary of the results of ABA testing for the Tigranes/Artavazdes Barren Rock and Table 4.7.3 shows the ABA summary for Erato Barren Rock.

Table 4.7.2: ABA Summary Tigranes/Artavazdes Barren Rock							
Barren Rock	**Statistics**	**Paste pH**	**AP**	**NP**	**Total S**	**Sulfide S**	**Sulfate S**
			$TCaCO_3$/kT	**$TCaCO_3$/kT**	**%**	**%**	**%**
Lower Volcanics	Mean	4.86	40.94	0.26	2.51	1.31	0.36
	Std. Dev.	1.07	60.00	1.67	2.57	1.92	0.55
Upper Volcanics	Mean	5.54	4.30	0.14	0.76	0.14	0.11
	Std. Dev.	0.70	21.39	0.85	1.40	0.68	0.20
Colluvium	Mean	5.79	0.87	0.20	1.07	0.03	0.13
	Std. Dev.	0.84	1.02	0.41	1.27	0.03	0.11

Table 4.7.3: ABA Summary - Erato Barren Rock								
Barren Rock	**Statistics**	**Paste pH**	**AP**	**NP**	**NAG pH**	**Total S**	**Sulfide S**	**Sulfate S**
			TCaCO3/kT	**TCaCO3/kT**		**%**	**%**	**%**
Lower Volcanics	Mean	5.00	27.44	0.38	4.28	2.16	0.88	0.38
	Std. Dev.	1.04	49.26	0.96	1.12	2.23	1.58	0.60
Upper Volcanics	Mean	5.30	5.48	0.27	4.72	0.83	0.18	0.11
	Std. Dev.	0.60	24.62	0.85	0.50	1.43	0.79	0.15
Colluvium	Mean	5.75	5.33	1.08	4.92	1.69	0.17	0.20
	Std. Dev.	0.19	11.19	0.86	0.15	2.42	0.36	0.28

Table 4.7.2 and Table 4.7.3 identify that the LV formation has the highest potential for ARD generation with an average sulphide sulphur content of 1.3% for the Tigranes and Artavazdes ore body, and 2.1% for the Erato ore body. The Upper Volcanics have some trace sulphides, but its oxidized nature and low total sulphide concentration (around 0.15%) make it so the low AGP of the VC does not realize itself as ARD (see Section 4.7.11) The colluvium, a low-volume waste type, does not have significant acid generating potential.

Table 4.7.4 shows the typical guidelines for determining which samples have ARD potential based on the ABA results.

Table 4.7.4: Screening Guidelines for Acid Generation Potential Prediction		
Material Designation:	**Comparative Criteria**	
	NNP ($TCaCO_3$/kT)	**NPR**
Potentially Acid-Generating (PAG)	< -20	< 1
Uncertain	-20 < NNP < 20	1 < NPR < 2
Non Potentially Acid Generating (NAG)	> 20	> 2
Reference: (INAP, 2009)		

The NNP is total NP minus total AP. The NPR is the ratio of NP to AP. Figure 4.6.9 shows the results of the screening criteria in graphical format.

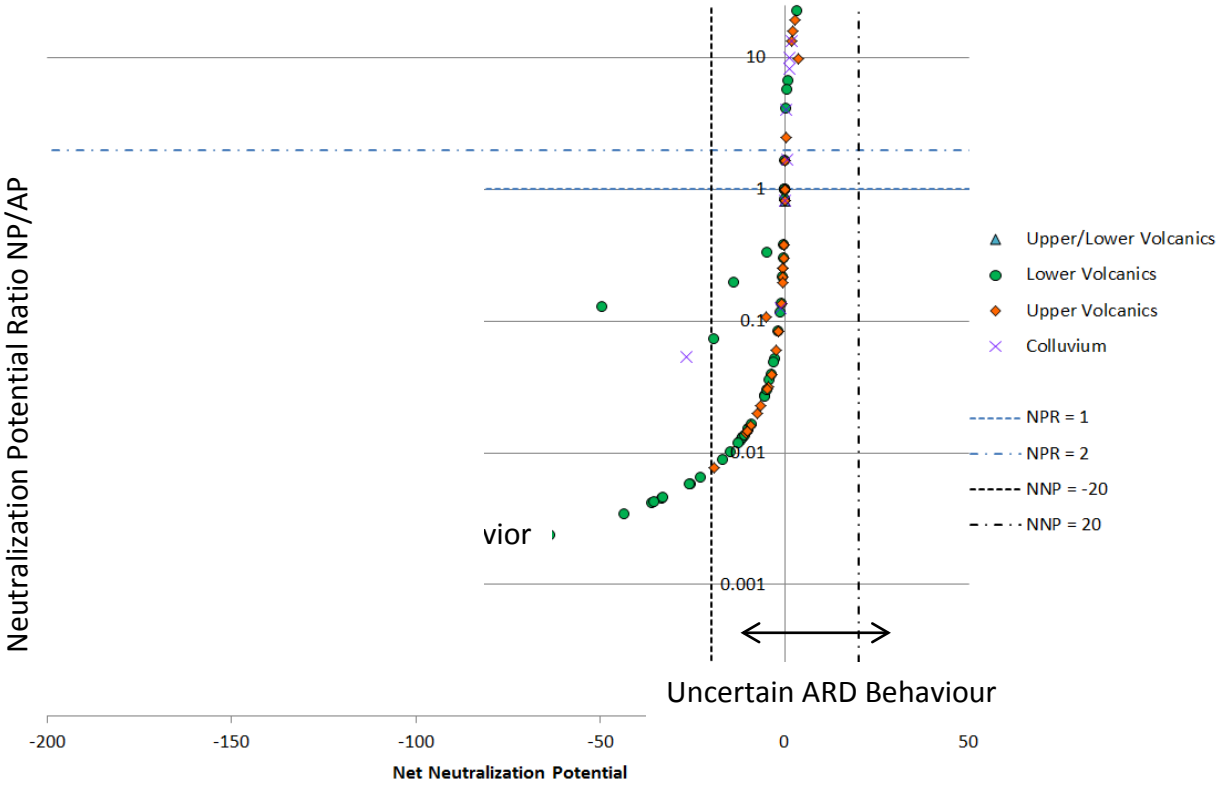

Figure 4.7.1: NNP vs. NPR for Tigranes/Artavazdes and Erato Barren Rock

As demonstrated in Figure 4.7.1, all of the Upper Volcanics samples fall within the "uncertain" range. This signifies that kinetic testing is required to determine if these samples have ARD generation potential. Despite the fact that good portion of the LV samples also fall in the uncertain range, the ABA testing confirms that the LV is an acid-generating rock type.

4.7.2 Acid-Base Accounting: Spent Ore

The spent ore is also a mine waste product and has the potential to produce ARD. The Project conducted ABA tests on spent ore from the Tigranes/Artavazdes pit and the Erato pit (see Table 4.7.5 and Table 4.7.6).

Table 4.7.5: ABA Results - Tigranes/Artavazdes Spent Ore (includes one Erato sample)					
Sample	**Total Sulfur**	**Acid Soluble Sulfate**	**Sulfide Sulfur**	**AP**	**NP**
	%	**%S**	**%**	**T $CaCO_3$/kT**	**T $CaCO_3$/kT**
MPF	0.04	0.02	0.02	0.63	3.06
GSN	0.58	0.05	0.53	16.50	4.31
FG	0.37	0.06	0.31	9.59	2.69
SB	0.38	0.04	0.34	10.66	2.31
MC068[1,2]	1.15	0.03	1.13	35.16	1.37
MC070[1]	0.70	0.05	0.65	20.22	2.50
MC071[1]	0.38	0.01	0.37	11.63	0.69
Notes: 1. Composite sample 2. Erato sample					

Table 4.7.6: ABA Results - Erato Spent Ore					
Sample	**Total Sulphur**	**Acid Soluble Sulphate**	**Sulfide Sulphur**	**AP**	**NP**
	%	**%S**	**%**	**T $CaCO_3$/kT**	**T $CaCO_3$/kT**
DDA-030	0.95	0.24	<0.01	0.31	0.30
DDA-030	0.14	0.11	<0.01	0.31	0.30
DDA-278	0.74	0.20	0.10	3.13	0.30
DDA-276	1.75	0.32	0.09	2.81	0.30
DDA-290	0.00	0.02	<0.01	0.31	0.30
DDA-340	0.53	0.24	<0.01	0.31	0.30

Based on the generally low sulphide sulphur levels, the 100% VC composition of the spent heap, and the abundant residual alkalinity present within the heap leach, it was determined that the spent ore is not an ARD risk.

4.7.3 Acid-Base Accounting: Borrow Materials

Four LV samples and one scoria sample were submitted for geochemical characterization to assess their suitability as potential site borrow materials. Table 4.7.7 provides a summary of the results of the borrow materials testing.

Table 4.7.7: ABA results for Borrow Materials						
Sample ID	**Lithology**	**NNP**	**NPR**	**Sulphide Sulphur (%)**	**NAG pH**	**Paste pH**
BH-305	LV	-0.10	0.83	0.02	5.44	6.65
BH-303	LV	-36.30	0.01	1.16	2.34	4.36
BH-307	LV	1.90	2.73	0.03	5.54	5.54
BH-308	LV	-31.90	0.01	1.02	4.89	5.63
BH-312	Scoria	18.00	60.00	0.01	5.92	8.59

Results indicate that LV should not be used as construction materials due to an ARD and metal leaching potential, unless other mitigation measures are implemented. Scoria, however, appears suitable, although additional characterization work is recommended, as only one sample was included in the testing programme. Some in-pit waste materials are also suitable as construction material. The Upper Volcanics and Colluvium lithologic groups contain geochemically suitable construction

4.7.4 Metals Leaching Potential Summary

An estimate of potential metal leaching behaviour of Amulsar barren rock has been summarised in Table 4.7.8.

Table 4.7.8: SPLP Leaching Summary - Tigranes/Artavazdes and Erato Barren Rock				
Parameter	**Units**	**Arpa Type II Standards**	**Tig/Art SPLP Results (avg)**	**Erato SPLP Results (avg)**
Ammonia as N	mg/L	0.4	0.102	0.172
Arsenic	mg/L	0.02	0.011	0.0007
Barium	mg/L	0.028	**0.027**	**0.073**
Biochemical Oxygen Demand	mg/L		2	2
Cadmium	mg/L	0.001	**0.002**	0.0007
Chemical Oxygen Demand	mg/L		8.2	5.489
Chromium	mg/L	0.011	0.006	0.002
Copper	mg/L	0.021	0.19	**1.837**
Cyanide (total)	mg/L		0.01	0.01
Cyanide (free)	mg/L		0.005	0.01
Cyanide (WAD)	mg/L		0.01	0.01
Final Fluid pH	pH units		5.953	5.25
Hexavalent Chromium	mg/L		0.012	0.012
Iron	mg/L	0.072	**3.423**	**3.002**
Lead	mg/L	0.0101	0.008	0.0005

Table 4.7.8: SPLP Leaching Summary - Tigranes/Artavazdes and Erato Barren Rock				
Parameter	**Units**	**Arpa Type II Standards**	**Tig/Art SPLP Results (avg)**	**Erato SPLP Results (avg)**
Manganese	mg/L	0.012	**0.04**	**0.025**
Mercury	mg/L		0.0002	0.000045
Nickel	mg/L	0.0103	**0.019**	**0.012**
Nitrate/Nitrite as N	mg/L		0.182	0.159
Orthophosphate as P	mg/L		0.01	0.01
Selenium	mg/L	0.02	**0.04**	0.0004
Sulphate as SO4	mg/L		28.273	35.938
Total Suspended Solids	mg/L	6.8		5
Zinc	mg/L	0.1	0.071	0.047

The Net Acid Generating (NAG) effluent test is a test of the effluent from the full oxidation of the sample using hydrogen peroxide. This analysis represents the worst-case for metals leaching potential using aggressive oxidation conditions (see Table 4.7.9).

Table 4.7.9: NAG Effluent Summary - Tigranes/Artavazdes and Erato Barren Rock				
Parameter	**Units**	**Arpa Type II Standards**	**Tig/Art NAG Results (avg)**	**Erato NAG Results (avg)**
Arsenic	mg/L	0.02	0.003	0.001
Barium	mg/L	0.028	**0.045**	**0.109**
Boron	mg/L		0.04	0.003
Cadmium	mg/L	0.001	**0.003**	0.0008
Chloride	mg/L	6.88	0.578	1.162
Chromium	mg/L	0.011	**0.042**	**0.021**
Copper	mg/L	0.021	**0.272**	**0.453**
Iron	mg/L	0.072	**55.144**	**9.251**
Lead	mg/L	0.0101	0.003	0.0009
Manganese	mg/L	0.012	**0.129**	**0.058**
NAG pH	pH units		3.728	4.342
Nickel	mg/L	0.0103	**0.059**	**0.011**
Selenium	mg/L	0.02	**0.049**	0.007
Sulfate as SO_4	mg/L		379.003	83.273
Zinc	mg/L	0.1	0.087	0.015

The analysis demonstrates that there is potential for metals leaching for barium, copper, iron, manganese, nickel, selenium, and sulphate. Chromium and cadmium were only found in trace amounts in the NAG effluent test, and were excluded from concern.

4.7.5 Kinetic Geochemical Testing

Long-term humidity cell geochemical kinetic tests were performed on Amulsar barren rock[9]. This test produces an over-estimate of the acid generation potential and metals leaching potential of a rock over time due to the following issues:

- The cells are held at a constant temperature of 20°F;
- The cells are kept at 100% humidity for a week, then flushed with 1L of distilled and deionized water; and
- The cells require a ¼ inch crush size, far smaller than in Run of Mine (ROM) waste.

Despite these limitations, long-duration kinetic cell tests provide a laboratory conditions to determine the ARD behaviour of rock types. It is generally accepted that a year of kinetic cell testing can prove beyond reasonable doubt that a rock sample will or will not generate acid. The test is a logical extension of the static testing because it demonstrates empirically whether the potential determined in the ABA testing will be reached in site conditions.

4.7.6 ARD Geochemical Reaction Kinetics

The kinetics of an ARD reaction are critical in defining the environmental impacts. Two different chemical reactions typically form ARD from the oxidation of pyrite.

Equation 1 involves the oxidation of pyrite in the presence of water:

$$FeS_2 + 7/2O_2 + H_2O = Fe^{2+} + 2SO_4^{2-} + 2H^+ \text{ [1] } ^{10} \text{ (INAP, 2009)}$$

This reaction commonly occurs at the Amulsar site. However, in the kinetic cells, a second reaction dominated the ARD behaviour of some cells later in the testing period. This equation involves the oxidation of pyrite by ferric iron (Fe3+). This reaction is much faster, and has a higher stoichiometric ratio between pyrite and acidity (listed as H+), Equation 2:

$$FeS_2 + 14Fe^{3}+ + 8H_2O = 15Fe^{2}+ + 2SO_4^{2}- + 16H^+ \text{ [2]}^{10} \text{ (INAP, 2009)}$$

[9] ASTM D5744-07e1. (2007). Standard Test Method for Laboratory Weathering of Solid Materials Using a Humidity Cell. *American Society for Testing and Materials*

[10] Global Acid Rock Drainage Guide. *International Network on Acid Prevention* INAP. (2009).

The reaction is catalyzed by the bacteria *Thiobacillus ferroxidans*. In subsequent sections, the changeover from ARD dominated by Equation 1 to ARD dominated by Equation 2 is referred to as: "ferric iron oxidation" because ferric iron is acting as a reactant in the oxidation of pyrite.

4.7.7 Humidity Cell Results

Figure 4.7.2 shows the pH of the kinetic cell rinsate over time, Figure 4.7.3 shows sulphate production over time, and Figure 4.7.4 shows iron production over time.

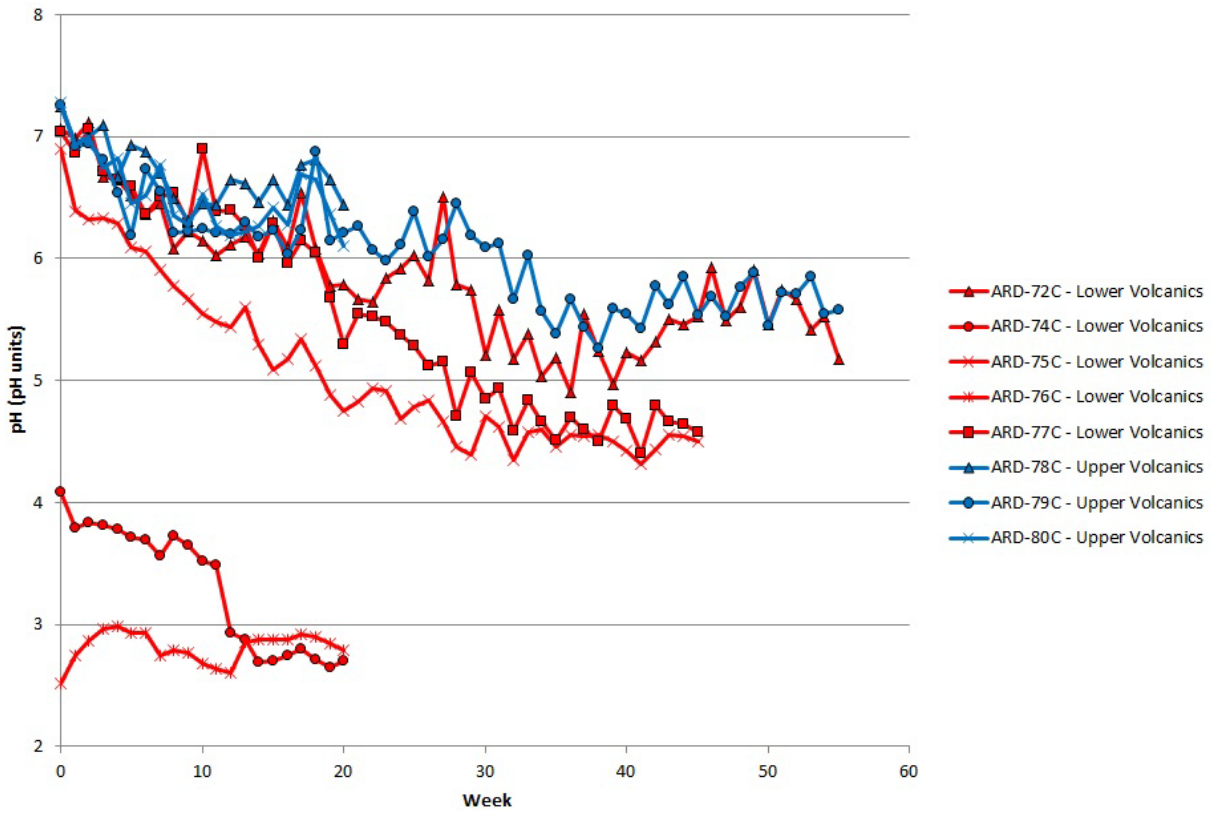

Figure 4.7.2: pH vs. Time in Kinetic Cell Tests

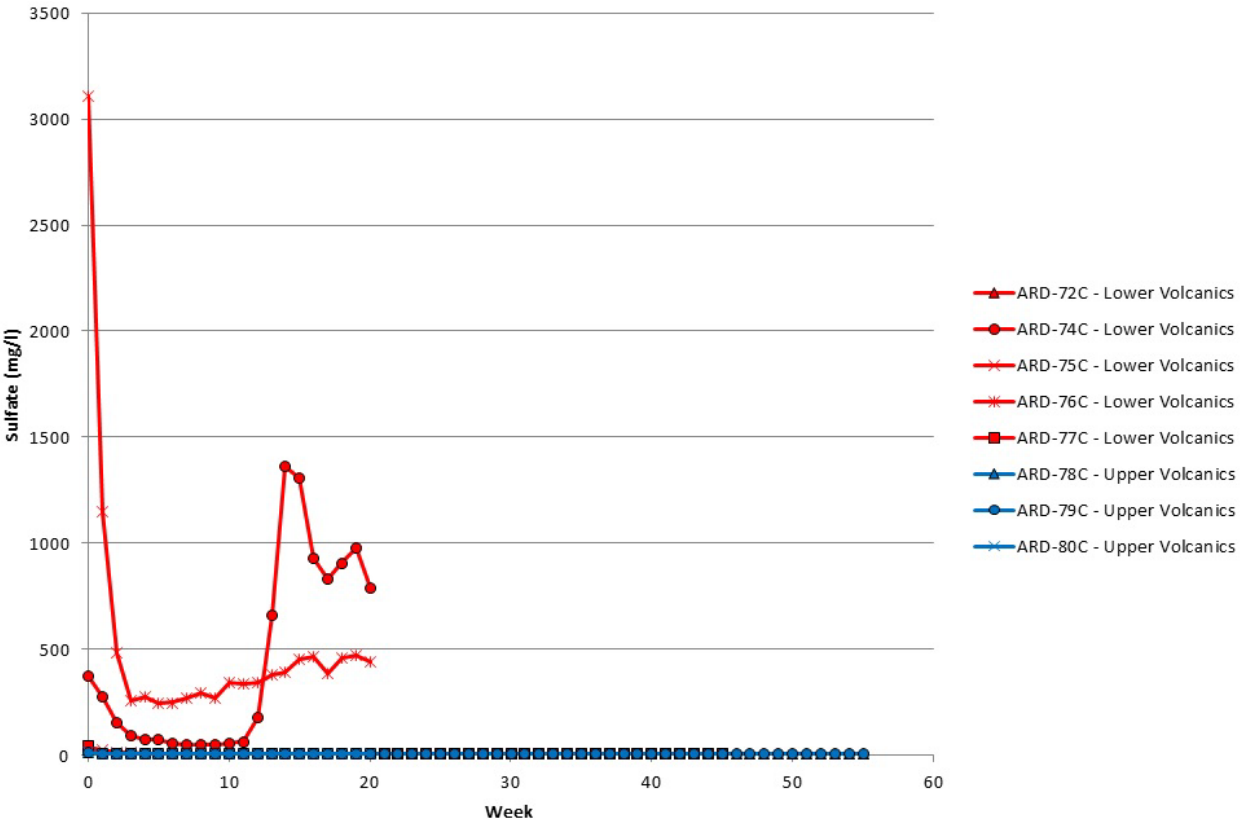

Figure 4.7.3: Sulphate vs. Time in Kinetic Cell Tests

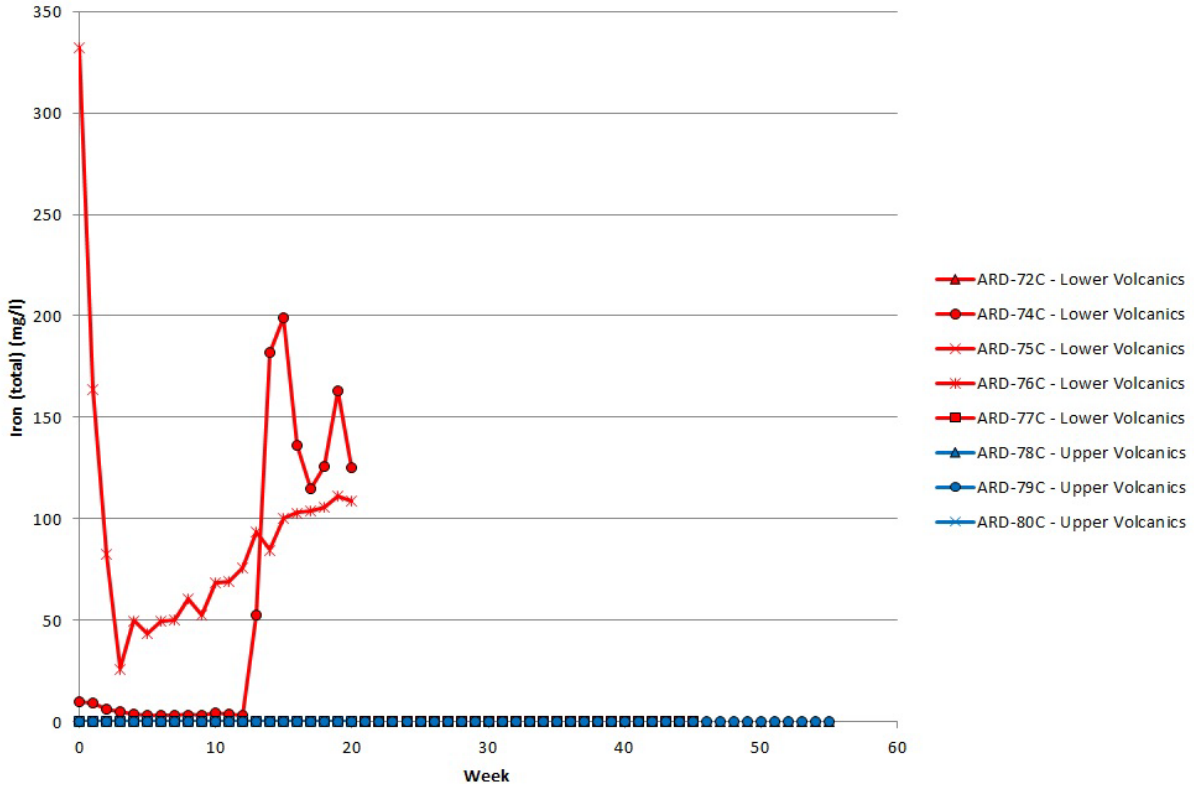

Figure 4.7.4: Iron vs. Time in Kinetic Cell Tests

It is clear from Figure 4.7.2 through Figure 4.7.3 that the ARD potential of the VC does not translate into ARD generation despite the "uncertain" nature of the ABA testing ("uncertain" as defined the analysis in Table 4.7.4). It is also clear that three of the five LV samples generate no significant sulphate or iron in the humidity cell rinsate (the symbols are obscured behind the VC line in Figure 4.7.3 and Figure 4.7.4).

The kinetic testing results reveal three different categories of LV samples tested.

- Samples that were oxidized prior to testing;
- A sample that converted to ferric iron oxidation; and
- Samples resistant to ferric iron oxidation.

These samples are discussed below.

4.7.8 Oxidized LV Samples

ARD-76C was heavily oxidized prior to arriving at the lab. This sample shows the worst-case potential of Amulsar waste, but has little value in determining reaction kinetics.

4.7.9 Sample ARD-74C

ARD 74C is the most useful sample in the sample dataset. For the first 12 weeks of the test, the cell oxidizes in the presence of oxidation (see Equation 1).

After 12 weeks, ferric iron oxidation begins and the rinsate has reduced pH, increased sulphate concentrations, and increased iron concentrations (Equation 2).

4.7.10 LV Samples Resistant to Ferric Iron Oxidation

Three of the five LV kinetic cells showed strong resistance to the formation of ferric iron oxidized ARD. These samples produce consistently mild (pH greater than 4.5) ARD with low sulphate and iron concentrations despite long-duration testing.

4.7.11 Observed Geochemistry

Two mine waste piles are already present within the Project footprint. They are within two of the sites studied for alternatives (see Chapter 5) and known as Site 27 and Site 13 (see Appendices 5.2 and 5.3). These rock piles result from uranium exploration undertaken in the 1950s. The waste piles are made of LV rock and show similar geologic and geochemical

characteristics to the mine waste from the Amulsar pits including sulphidisation, argillization, and occasional silicification. These rock produce ARD; however, the severity of ARD produced can be classified as moderate to mild. It has a water quality signature similar to LV samples that have not undergone ferric iron oxidation (see Section 4.7.6). Samples of the Site 13 and Site 27 mine waste were collected and analyzed. The results, when compared to the total population of LV, are shown in Table 4.7.10.

This updated table counts detection level results as zero for the LV calculations.

Table 4.7.10: Site 13 and 27 Mine Waste ABA Compared with Amulsar Pits

Barren Rock	Sample Count	Statistics	AP	NP
			T/KT	
LV	57	Average	37.44	0.29
		Median	5.60	0.00
		St. Dev.	57.58	1.52
		Range	0 to 204	0 to 14.18
Sites 13 and 27	4	Average	10.62	-0.75
		Median	7.34	-0.95
		St. Dev.	8.70	0.50
		Range	4.37 to 23.43	-1.1 to 0

The average from the LV dataset in the pit is higher, and the median is lower than the Site 13 and Site 27 mine waste. The rock from this exploration programme is not significantly different from LV samples recovered from the footprint of the Tigranes, Artavazdes and Erato pits despite the fact that the rock has been exposed to air and has been subject to oxidation for sixty years.

It is considered, therefore that the exposed rock is relevant to the geochemical study for the Project, and can be considered a long-term on-site kinetic cell test that can inform the conceptual model and management plan.

Table 4.7.11 shows the leachate water quality from the exposed rock in Sites 13 and Site 27.

Table 4.7.11: Site 13 and 27 Mine Waste Leachate, May 2014							
Constituent	**Unit**	**WK 10**	**WK 14**	**SPLP**	**Exposed rock stockpiles Waste**		**Site 13 Baseline Surface Water**
		ARD 74C			**Site 13**	**Site 27**	
pH	pH units	3.52	2.69	4.64	4.78	3.28	6.38
Acidity	mg/L as $CaCO_3$	59	1210	N.S.	15.10	102.00	<D.L.
Sulfate	mg/L	59	1360	46	12.60	43.70	35.70

This leachate water quality has a higher pH, lower sulphate, and lower total acidity than what was observed in the later weeks of the ARD 74C humidity cell test (see Figure 4.7.2 to Figure 4.7.4). It is clear that after 60 years, the waste in the pile has not shifted over into ferric iron oxidation dominated ARD reaction kinetics.

As a result, the waste rock shows that the LV rock has some natural suppression agent that prevents the formation of ferric iron oxidation. The suppression could be any or all of the below:

- *Thiobacillius ferrooxidans* has a much slower sulphide reaction rate in cold climates[11];
- The exposed rock argillic texture (with approximately 10% clay content) inhibits the flow of oxygen within the pile, and therefore, oxidation; and/or
- The LV mineral has some residual natural resistance to ferric iron oxidation that is only overcome in the extraordinary conditions of a long-term humidity cell test.

This natural resistance is a critical to the characterization of Amulsar barren rock and the design of the BRSF (see Appendix 3.1)

[11] Weathering of Waste Rock in Different Cimatic Condtions -- A Kinetic Freeze/Thaw and Humidity Cell Experiment. Sartz, L. (2011). *International Mine Water Association Congress.* Aachen, Germany: IMWA

4.7.12 Summary of Characterization

The characterization of mine waste reveals the following:

- The VC is non-acid generating, despite the existence of trace AP;
- The VC has leachate slightly lower than circumneutral, likely due to the weathering of alunite. The weathering of alunite is not significant to water quality due to the very slow reaction kinetics and low total acidity produced[12];
- The LV is acid generating, but appears to be resistant to ferric iron oxidation under field conditions;
- Colluvium is not acid generating; and
- There is potential for metals leaching for copper, iron, manganese, selenium, and sulphate.

Further details of the test work and test results are provided in Appendix 8.19.

Summary

Extensive geological exploration has been undertaken at the Amulsar Project. The Amulsar deposit is associated with a complex alteration system and a structural complexity that has not been observed in this sub-region, and forms part of the Amulsar Ridge – a geologically anomalous feature within the wider geological context. The main rock types include Upper Volcanics, Lower Volcanics, and two different local intrusive suites.

The Project is in a seismically active region, but there is no geomorphic evidence for traces of faults or other tectonic geomorphology within the footprint of the Project. Thus there is low risk of a surface fault rupture within the Project area.

Various rock types at the Project have potential to generate acid rock drainage. The main potential sources are due to water coming into contact with exposed Lower Volcanics.

[12] *Summary of Geochemical Charaterization and Water Quality Prediction -- Revised: Amulsar Gold Project.* GRE. (2014). Denver, Colorado: Global Resource Engineering